High-order FDTD methods for transverse electromagnetic systems in dispersive inhomogeneous media

Shan Zhao

Department of Mathematics, University of Alabama, Tuscaloosa, Alabama 35487, USA (szhao@bama.ua.edu)

Received June 8, 2011; accepted July 18, 2011;
posted July 22, 2011 (Doc. ID 148966); published August 15, 2011

This Letter introduces a novel finite-difference time-domain (FDTD) formulation for solving transverse electromagnetic systems in dispersive media. Based on the auxiliary differential equation approach, the Debye dispersion model is coupled with Maxwell's equations to derive a supplementary ordinary differential equation for describing the regularity changes in electromagnetic fields at the dispersive interface. The resulting time-dependent jump conditions are rigorously enforced in the FDTD discretization by means of the matched interface and boundary scheme. High-order convergences are numerically achieved for the first time in the literature in the FDTD simulations of dispersive inhomogeneous media. © 2011 Optical Society of America

OCIS codes: 000.4430, 160.2710, 260.2030.

Recently, much attention has been devoted to the development of efficient time-domain methods for solving Maxwell's equations in dispersive media, including the FDTD methods [1,2], finite element time-domain methods [3], discontinuous Galerkin time-domain methods [4–6], and so on. The success of these methods lies in the accurate implementation of the frequency-dependent material constitutive relations in the time domain. However, great challenges exist in all dispersive simulations on how to restore the accuracy reduction at the dispersive interface, where the wave solution loses its regularity in a complicated way.

To account for the nonsmoothness of wave solution at the dispersive interface, several dispersive FDTD algorithms [7–9] have been constructed by averaging the permittivity in the vicinity of the interface so that a smooth effective permittivity is produced for wave simulation. Consequently, the numerical convergence can be accelerated. On the other hand, it is well known in the computational electromagnetics literature [10] that a more accurate way to treat the material interface is to incorporate the physical jump conditions into the numerical discretization in a proper manner. The resulting interface schemes can deliver higher-order convergences irrespective of the presence of material interfaces [10–12]. However, to the author's knowledge, no rigorous interface scheme has ever been formulated for treating the dispersive interface. This is because, as to be shown in this Letter, the jump conditions at the dispersive interface could be time dependent—a difficulty that has not been encountered in the previous interface studies [10–12].

It is of great interest to develop higher-order interface methods for the dispersive interface. To this end, we present in this Letter a novel FDTD formulation for one-dimensional (1D) Maxwell's equations. Consider an x-directed, z-polarized transverse electromagnetic system in dispersive inhomogeneous media

$$\frac{\partial D_z}{\partial t} = \frac{\partial H_y}{\partial x}, \qquad \frac{\partial H_y}{\partial t} = \frac{1}{\mu}\frac{\partial E_z}{\partial x}, \tag{1}$$

where E_z and H_y are, respectively, electric and magnetic field components, and D_z is the electric displacement component. For dispersive media, the constitutive relation is better prescribed in the frequency domain, i.e., $\hat{D}_z = \hat{\epsilon}(\omega)\hat{E}_z$, in which the time-harmonic components are obtained via the Fourier transforms of the time-varying components.

For simplicity, we focus ourselves on the single-order Debye dispersion model

$$\hat{\epsilon}(\omega) = \epsilon_0\left[\epsilon_\infty + \frac{\epsilon_s - \epsilon_\infty}{1 + j\omega\gamma}\right], \tag{2}$$

where ϵ_0, ϵ_s, and ϵ_∞ are, respectively, permittivities of free space, at static frequency, and at high frequency limit. Here ω is the angular frequency and γ is the relaxation time constant. The auxiliary differential equation approach [1] is used to represent the constitutive Eq. (2) in time domain

$$\gamma\frac{\partial D_z}{\partial t} + D_z = \epsilon_0\epsilon_\infty\gamma\frac{\partial E_z}{\partial t} + \epsilon_0\epsilon_s E_z. \tag{3}$$

Equations (1) and (3) form a closed system. The classical dispersive FDTD method [1] can be formulated by discretizing such a system.

The proposed FDTD formulation is driven by the consideration of the dispersive interface. Consider a 1D domain $x \in [a, b]$ with $\mu = \mu_0$ throughout. Assume an interface location at $x = d$ and the left subdomain $[a, d)$ being vacuum with $\epsilon = \epsilon_0$, while the right subdomain $[d, b]$ is a dispersive medium. Define function limits and jump of function $u(x)$ at $x = d$ to be $u^+ := \lim_{x\to d^+} u$, $u^- := \lim_{x\to d^-} u$, and $[u] := u^+ - u^-$. To unify the notation, we assume Eq. (2) in vacuum as well with $\epsilon_s^- = \epsilon_\infty^- = 1$. Then γ^- is a free parameter so that we can assume $\gamma = \gamma^- = \gamma^+$ being a constant throughout $[a, b]$.

We have the ordinary jump conditions [11] for E_z

$$[E_z] = 0, \qquad \left[\frac{\partial E_z}{\partial x}\right] = 0, \tag{4}$$

which can be simply handled by the previous interface schemes [10–12]. For H_y, we have continuity condition $[H_y] = 0$. However, the first-order jump condition for H_y is physically unknown. We overcome this difficulty by solving a supplementary ordinary differential equation

(ODE). Assume $[D_z] = \psi(t)$ for some unknown function $\psi(t)$. We have $[\partial H_y/\partial x] = [\partial D_z/\partial t] = \psi'(t)$. By taking jumps for (3), we obtain an ODE

$$\gamma\psi'(t) + \psi(t) = \epsilon_0\gamma[\epsilon_\infty \dot{E}_z] + \epsilon_0[\epsilon_s E_z], \tag{5}$$

where $\dot{E}_z = \partial E_z/\partial t$. To facilitate the solution of the ODE (5), we propose to utilize $\dot{E}_z$ instead of D_z to form a closed Maxwell system:

$$\frac{\partial \dot{E}_z}{\partial t} = -\frac{\epsilon_s}{\epsilon_\infty\gamma}\dot{E}_z + \frac{1}{\epsilon_0\mu_0\epsilon_\infty}\frac{\partial^2 E_z}{\partial x^2} + \frac{1}{\epsilon_0\epsilon_\infty\gamma}\frac{\partial H_y}{\partial x}, \tag{6}$$

$$\frac{\partial E_z}{\partial t} = \dot{E}_z, \qquad \frac{\partial H_y}{\partial t} = \frac{1}{\mu_0}\frac{\partial E_z}{\partial x}. \tag{7}$$

In the proposed higher-order FDTD methods, the ODE (5) and Maxwell's Eqs. (6) and (7) will be time integrated via the classical fourth-order Runge–Kutta method [11]. We note that other standard explicit or implicit time stepping methods may also be used for time integration. In the present study, at each time step $t_k = k\Delta t$, the right-hand side of (5) can be calculated as $g(t_k) := \epsilon_0\gamma(\epsilon_\infty^+ - \epsilon_\infty^-)\dot{E}_z^-(t_k) + \epsilon_0(\epsilon_s^+ - \epsilon_s^-)E_z^-(t_k)$. Here $E_z^-(t_k)$ and $\dot{E}_z^-(t_k)$ are approximated via one-sided extrapolation based on several function values of $E_z(t_k)$ and $\dot{E}_z(t_k)$ from the left of the interface. With $g(t_k)$, one can compute $\psi(t_k)$ and $\psi'(t_k)$ at each time step t_k.

With $\psi'(t)$ being accurately estimated, a matched interface and boundary (MIB) method [11,12] is utilized to impose jump conditions at the dispersive interface, i.e.,

$$[H_y] = 0, \qquad \left[\frac{\partial H_y}{\partial x}\right] = \psi'(t), \tag{8}$$

for H_y and (4) for E_z. In particular, a uniform staggered grid system is used for E_z and H_y on the domain $[a, b]$. The standard $(2M)$th order central FDTD approximation [11] is employed for spatial discretization, with M being the half stencil bandwidth. In the MIB algorithm, when the FDTD stencil refers to function values from the other side of the interface, fictitious values instead of original function values will be supplied. In general, to support a $(2M)$th order FDTD approximation, M fictitious nodes from the positive side and M ones from the negative side of the interface are required for E_z. So does H_y.

Since the jump conditions (4) and (8) are decoupled, we consider only the MIB scheme for (8) here. In the first step of the MIB scheme [11,12], H_y^- and $\partial H_y^-/\partial x$ are discretized by using L original H_y values from the negative side and one fictitious value of H_y from the positive side. With the similar discretization for H_y^+ and $\partial H_y^+/\partial x$, (8) becomes two algebraic equations. Solving them, one attains two fictitious values for H_y. The MIB scheme iteratively enforces the jump condition (8) [11,12] so that $2M$ fictitious values can be obtained after M iterations. These fictitious values of H_y will depend on $2L$ function values of H_y and the nonhomogeneous value $\psi'(t)$. The jump condition (4) for E_z can be similarly treated.

We validate the proposed MIB time-domain (MIBTD) methods by considering an air–water interface. We choose a domain with $a = 0$ mm, $b = 30$ mm, and $d = 7.5\pi$ mm. Similar to [2], we assume $\epsilon_s = 81$, $\epsilon_\infty = 1.8$, and $\gamma = 9.4$ ps for the water. An incident pulse of the form $E(t) = \exp(-(x + 15 - c_0 t)^2/(2\tau^2))$ is employed as the boundary condition at $x = a$. Here $\tau = 2.5$ mm and c_0 is the speed of light in air. The boundary condition at $x = b$ is assumed to be perfectly conducting for simplicity. A high-order boundary closure scheme presented in [13] is employed to treat such a boundary.

We first test the second-order MIBTD or MIBTD2 for calculating the reflection coefficient of the air–water interface. For the MIBTD2, we choose $M = 1$ and $L = 2$. The number of nodes for E_z is chosen as $N = 801$ and the time increment is $\Delta t = 0.025$ ps for $N_t = 10000$ steps. Numerical values of E_z are tracked at one location near the left boundary and another to the left of the interface. Through a proper truncation, this yields two time histories for incident and reflected pulse, respectively. The reflection coefficient can then be calculated as the ratio of the Fourier transform of the reflected wave over that of the incident wave. The reflection coefficient of the MIBTD2 is plotted against the analytical one [2] in Fig. 1. A good agreement over various frequencies is clearly seen.

To fully demonstrate the potential of higher-order MIBTD methods, we consider next a rigorous convergence analysis. The parameters for higher-order MIBTD are chosen as: $(M, L) = (2, 4)$ and $(3,6)$, respectively, for the MIBTD4 and MIBTD6. We select the stop time to be $t = 140$ ps, which is short enough such that both reflected and transmitted pulses have not reached the boundaries, see Fig. 2. We choose the number of time steps to be $N_t = 10000$ in all computations. The corresponding $\Delta t = 0.014$ ps is small enough so that the approximation errors are guaranteed to be mainly produced by the spatial discretizations. To benchmark the numerical results, we generate a reference solution by employing the MIBTD6 with a very dense grid $N = 12801$. Convergence analysis can then be conducted by considering mesh refinements using nodes that are also covered in the reference solution. We note that since the H_y nodes are staggered to the E_z nodes, the present convergence analysis is not applicable to H_y.

The maximum errors in E_z of the MIBTD methods are depicted in Fig. 3. For a comparison, the results of the classical dispersive FDTD [1] are also shown. In all cases, the numerical errors based on different mesh size N are plotted as dashed lines. A linear least-squares fitting [12]

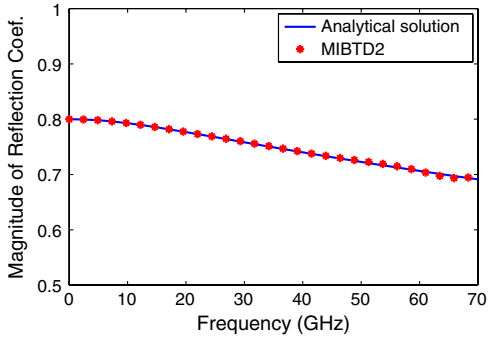

Fig. 1. (Color online) Reflection coefficient at an air–water interface.

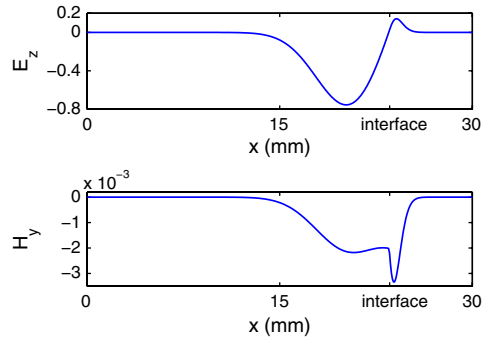

Fig. 2. (Color online) MIBTD6 solution with $N = 401$ at $t = 140$ ps. Top, E_z; bottom, H_y.

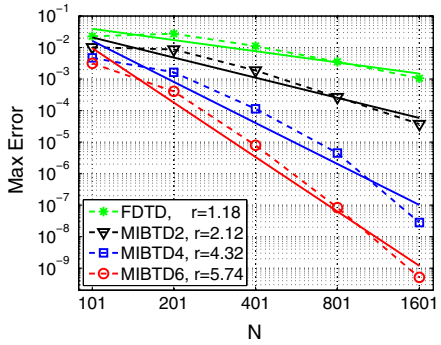

Fig. 3. (Color online) Numerical convergence tests of E_z.

is then conducted in the log-log scale. The fitted convergence lines are shown as solid lines in Fig. 3. Moreover, the fitted slope essentially represents the numerical convergence rate r of the scheme. The conventional FDTD algorithm attains $r = 1.18$, because it degrades to the first order of accuracy due to the loss of solution regularities at the dispersive interface [11]. In particular, it is clear from Fig. 2 that E_z is C^1 continuous, but H_y is only C^0 continuous. Higher-order convergence can be achieved only when special interface treatments, such as the proposed MIB schemes, are incorporated in the discretization. In the present study, the numerical order r of the MIBTD2, MIBTD4, and MIBTD6 methods is found to be 2.12, 4.32, and 5.74, respectively, which confirms the theoretical orders of two, four, and six.

We finally present an efficiency study. Based on the same mesh size N and N_t, the MIBTD methods need more execution time than the FDTD scheme. However, the MIBTD methods can be more efficient, if the same accuracy level is required to be achieved by the FDTD scheme. For example, if one specifies the maximum error being at most 5.0×10^{-5}, the MIBTD2, MIBTD4, and MIBTD6 can accomplish this goal by choosing N to be 1601, 801, and 401, respectively. By using a fixed $N_t = 10000$, the execution time for MIBTD2, MIBTD4, and MIBTD6, is 3.99, 2.21, and 1.25 s, respectively. Nevertheless, a very large $N = 102401$ has to be used in the FDTD for the desired accuracy. Moreover, due to time stability constraint, a very large $N_t = 160000$ has to be used for time integration. Such an FDTD simulation costs 243.71 s. Thus, the MIBTD6 scheme is about 195 times more efficient that the FDTD method.

In summary, we have proposed a novel interface formulation for treating Debye dispersive interface in 1D. The time-dependent jump conditions are coupled with Maxwell's equations via a supplementary ODE. Higher-order convergences are numerically achieved for the first time in the literature in the FDTD simulation of dispersive inhomogeneous media. The dispersive interface formulation for higher dimensions is currently under our investigation.

This work is supported in part by the National Science Foundation (NSF) grant DMS-1016579 and by a University of Alabama Research Grants Committee Award.

References

1. R. M. Joseph, S. C. Hagness, and A. Taflove, Opt. Lett. **16**, 1412 (1991).
2. O. P. Gandhi, B.-Q. Gao, and J.-Y. Chen, IEEE Trans. Microwave Theory Tech. **41**, 658 (1993).
3. J. Li, J. Comput. Appl. Math. **188**, 107 (2006).
4. T. Lu, P. Zhang, and W. Cai, J. Comput. Phys. **200**, 549 (2004).
5. Y. Q. Huang and J. Li, J. Sci. Comput. **41**, 321 (2009).
6. B. Wang, Z. Xie, and Z. Zhang, J. Comput. Phys. **229**, 8552 (2010).
7. Y. Zhao and Y. Hao, IEEE Trans. Antennas Propag. **55**, 3070 (2007).
8. A. Deinega and I. Valuev, Opt. Lett. **32**, 3429 (2007).
9. A. Mohammadi, T. Jalali, and M. Agio, Opt. Express **16**, 7397 (2008).
10. J. S. Hesthaven, Adv. Imaging Electron Phys. **127**, 59 (2003).
11. S. Zhao and G. W. Wei, J. Comput. Phys. **200**, 60 (2004).
12. S. Zhao, J. Comput. Phys. **229**, 3155 (2010).
13. S. Zhao and G. W. Wei, Int. J. Numer. Methods Eng. **77**, 1690 (2009).